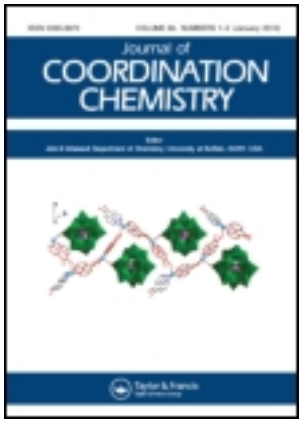

Journal of Coordination Chemistry
Publication details, including instructions for authors and subscription information:
http://www.tandfonline.com/loi/gcoo20

Dinuclear copper(II) complexes with tetraacetylpropane bridge; synthesis and solvatochromism study

Hamid Golchoubian [a b], Ehsan Rezaee [a b], Giuseppe Bruno [c] & Hadi Amiri Rudbari [d]

[a] Department of Chemistry, University of Mazandaran, Babolsar, Iran

[b] Department of Chemistry, Mohammad Reza Hariri Science Foundation, Babol, Iran

[c] Dipartimento di Chimica Inorganica, Università di Messina, Messina, Italy

[d] Faculty of Chemistry, University of Isfahan, Isfahan, Iran

Accepted author version posted online: 13 May 2013.Published online: 11 Jun 2013.

To cite this article: Hamid Golchoubian, Ehsan Rezaee, Giuseppe Bruno & Hadi Amiri Rudbari (2013) Dinuclear copper(II) complexes with tetraacetylpropane bridge; synthesis and solvatochromism study, Journal of Coordination Chemistry, 66:13, 2250-2263, DOI: 10.1080/00958972.2013.801961

To link to this article: http://dx.doi.org/10.1080/00958972.2013.801961

Journal of Coordination Chemistry, 2013
Vol. 66, No. 13, 2250–2263, http://dx.doi.org/10.1080/00958972.2013.801961

Dinuclear copper(II) complexes with tetraacetylpropane bridge; synthesis and solvatochromism study

HAMID GOLCHOUBIAN*†‡, EHSAN REZAEE†‡, GIUSEPPE BRUNO§ and HADI AMIRI RUDBARI¶

†Department of Chemistry, University of Mazandaran, Babol-sar, Iran
†‡Department of Chemistry, Mohammad Reza Hariri Science Foundation, Babol, Iran
§Dipartimento di Chimica Inorganica, Università di Messina, Messina, Italy
¶Faculty of Chemistry, University of Isfahan, Isfahan, Iran

(*Received 3 January 2013; in final form 21 March 2013*)

Two new mixed-chelate dinuclear copper(II) complexes, $[Cu_2(tmen)_2(TAP)]X_2$ where tmen = *N,N,N′,N′*-tetramethylethylenediamine, TAP = tetraacetylpropane, and $X = ClO_4^-$ or BPh_4^-, were prepared and characterized by physicochemical and spectral (IR, UV–vis) data. The X-ray diffraction study of $[\{Cu(tmen)(CH_3CN)\}\{Cu(tmen)(ClO_4)\}(TAP)](ClO_4)$ demonstrated that coordination geometry around the copper centers is square pyramidal where axial position of one copper is occupied by a ClO_4^- and the second copper with acetonitrile. However, in solution, the resulting complexes display affinity for axial ligation so that the apical ligands are driven out by solvent molecules. The solvatochromism of the complexes was investigated in various organic solvents and was compared with that of the corresponding mononuclear complex $[Cu(tmen)(CH_3\text{-acac})]ClO_4$. A multi-parametric equation has been utilized to explain the solvent effect on the d–d transition of the complexes using SPSS/PC software. To explore the mechanism of the interaction between the solvent molecules and the complexes, different solvent parameters such as DN, AN, α, $E_T(30)$, π^*, and β using stepwise multiple linear regression method were employed. In pyridine, the original color of the solution changed over time due to removal of tmen chelates and substitution by pyridine in two successive steps.

Keywords: Solvatochromism; Tetraketonate; Dinuclear copper complex; Mixed-chelate complex; SMLR method

1. Introduction

The solvatochromism defines a reversible color change of materials due to changes in their solvents. β-Diketones are simple and highly efficient metal chelating ligands and their coordination properties have been investigated for a long time [1]. These ligands have been used for synthesis of different kinds of homo and heteroleptic complexes with different metal ions such as Cu(II), Ni(II), Fe(II) [2–5]. Among the vast collection of solvatochromic complexes, there are mixed-chelate copper(II) complexes that exhibit considerable and gradual color change over a wide range of solvent [6–10]. Due to their square planar structure, the origin of the solvatochromism phenomena in these

*Corresponding author. Email: h.golchobian@umz.ac.ir

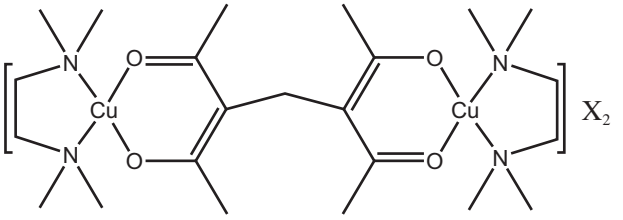

X = ClO_4 and BPh_4

Scheme 1. The prepared mixed-chelate dinuclear complexes.

compounds is usually the direct attachment of solvent onto metal center that is called the first type solvatochromism, while in the second type, indirect interactions between solvent and ligands in complexes are the origin of solvatochromism. The latter interaction usually occurs in coordinatively saturated complexes of octahedral structure. There are many reports about synthesis and solvatochromism of mononuclear copper(II) mixed-chelate complexes, [Cu(dike)(diamine)]X, in which the diamine stands for *N,N′*-polyalkylated ethylenediamine, "dike" as a β-diketonate and X different counter ions such as ClO_4^-, PF_6^-, etc. [11–14]. These complexes are soluble in a wide range of solvents, as require for solvatochromic compounds and show distinctive color changes [15–23]. In spite of various color changes, the color intensity of these complexes is low since the source of the color originates from the d–d transition of copper(II). Thus, syntheses of complexes with solvatochromic properties that contain higher molar extinction coefficient are particularly desirable since they can be used as Lewis acid-base color indicators [3], imaging [24], photo-switching [25], and sensor materials [26] and developing optical sensor materials to monitor pollutant levels in the environment [22]. In this regard, a series of mixed-chelate dinuclear complexes with β-diketone groups directly connected through their γ position were prepared and their solvatochromic properties studied [15]. The obtained results encouraged us to investigate effect of spacers like CH_2 between two β-diketone groups on the solvatochromism of the resulting dinuclear complex. This design causes two CuN_2O_2 mixed-chelate subunits to become skewed and steric crowding around copper increases, enhancing the solvatochromic property. Thus, two new dinuclear mixed-chelate copper(II) complexes, $[Cu_2(TAP)(tmen)_2]X_2$ (TAP = tetraacetylpropane; tmen = *N,N,N′,N′*-tetramethylethylenediamine; X = ClO_4, BPh_4), as illustrated in scheme 1 were synthesized and characterized and their solvatochromism behaviors studied.

There are a number of empirical scales for solvent polarity such as Dimorth and Reichardt's $E_T(30)$, Taft's (β, α, π^*), dielectric constant (ε) and Gutmann's donor (DN) and acceptor numbers (AN) that can be utilized to interpret solute–solvent interactions [27–31]. One or a combination of them might be effective in the observed solvatochromism of compounds. To ascertain the best model that describes the solvatochromic behavior of compounds a statistical method like multiple linear regression (MLR) can be applied. In this study, correlation between maximum wavenumber of the complexes and solvent parameters (DN, AN, $E_T(30)$, α, β, π^*) was studied using stepwise multiple linear regression (SMLR) method.

2. Experimental

2.1. *Materials and methods*

TAP [32] and [Cu(tmen)(CH_3-acac)](ClO_4) (**3**) [33] were prepared according to published procedures. All solvents were spectral grade and all other reagents were used as received. All samples were dried to a constant weight under a high vacuum prior to analysis. *Caution! perchlorate salts are potentially explosive and should be handled with appropriate care*. Conductance measurements were made at 25 °C with a Jenway 400 conductance meter on concentrations of 1.00×10^{-3}, 6.00×10^{-4}, 4.00×10^{-4}, and 2.00×10^{-4} M samples in selected solvents. Then, for each solvent, a curve was plotted by drawing the molar conductance versus concentration of sample. The curve was then extrapolated to infinitely dilute solution to obtain the molar conductance value. Infrared spectra (potassium bromide disk) were recorded using a Bruker FT-IR instrument. Electronic absorption spectra were measured using a Braic2100 model UV–Vis spectrophotometer. Elemental analyses were performed on a LECO 600 CHN elemental analyzer. Absolute metal percentages were determined by a Varian-spectra A-30/40 atomic absorption-flame spectrometer. The following solvents were used for solvatochromic study: dichloromethane (DCM), nitromethane (NM), nitrobenzene (NB), benzonitrile (BN), acetonitrile (AN), propionitrile (PN), acetone (Ac), tetrahydrofuran (THF), ethanol (EtOH), methanol (MeOH), dimethylformamide (DMF), dimethylsulfoxide (DMSO), pyridine (Py), and hexamethylphosphorictriamide (HMPA).

2.2. *Preparation of [{Cu(tmen)(CH_3CN)}{Cu(tmen)(ClO_4)}(TAP)](ClO_4) (1)*

To solution of *tmen* (6.6 mM, 1 mL), *TAP* (3.3 mM, 0.7 g), and Na_2CO_3 (3.3 mM, 0.34 g) in ethanol (15 mL) was slowly added $Cu(ClO_4)_2 \cdot 6H_2O$ (6.6 mM, 2.4 g) in water (15 mL). The resultant solution was allowed to stand overnight at room temperature. After partial concentration of the solution at room temperature, dark blue crystals precipitated that were collected by filtration. Appropriate single crystals for X-ray crystallography were grown by recrystallization from diffusion of diethyl ether into acetonitrile solution. The typical yield was 60%. Anal. calcd for $C_{23}H_{46}N_4O_{12}Cu_2Cl_2 \cdot H_2O$ (MW = 784.12 g M^{-1}): C, 35.12; H, 6.15; N, 7.12; Cu, 16.16. Found: C, 35.07; H, 6.24; N, 7.17; Cu, 16.02%. Selected IR data (ν/cm^{-1}): 1573 ν(C=O) (ketone), 1107 ν(Cl–O str.) (perchlorate), 624 ν(Cl–O bend.) (perchlorate).

2.3. *Preparation of [Cu_2(TAP)(tmen)$_2$](BPh_4)$_2$ (2)*

Complex **1** (0.17 g, 0.2 mM) was dissolved in 3 mL of methanol. To the resultant solution upon stirring was added a saturated solution of $NaBPh_4$ in water. A gray solid precipitated almost immediately that was collected, washed with water, and dried in vacuum. Yield: 80%. Anal. Calcd for $C_{71}H_{86}N_4O_4Cu_2B_2 \cdot 2H_2O$ (MW = 1242.56 g M^{-1}): C, 68.54; H, 7.29; N, 4.50; Cu, 10.21. Found: C, 69.00; H, 7.10; N, 4.67; Cu, 10.44%. Selected IR data (ν/cm^{-1}): 1564 ν(C=O) (ketone), 736 and 707 (tetraphenylborate).

Table 1. Crystal data and structure refinement for **1**.

Compound	[{Cu(tmen)(CH_3CN)}{Cu(tmen)(ClO_4)}(TAP)](ClO_4) (**1**)
Empirical formula	$C_{25}H_{49}Cl_2Cu_2N_5O_{12}$
Formula weight	809.60
Color	Dark blue
Temperature (K)	296(2)
Wavelength (Å)	0.71073
Crystal system	Triclinic
Space group	*P*−*1*
Crystal size (mm)	0.43 × 0.36 × 0.18
a (Å)	10.6856(2)
b (Å)	13.2534(2)
c (Å)	14.2142(2)
α (°)	69.3189(8)
β (°)	73.2277(8)
γ (°)	80.1156(9)
Volume (Å^3)	7015.4(5)
Z	2
Calculated density (Mg m^{-3})	1.496
F(0 0 0)	844
θ Range for data collection (°)	1.88–25.99
Index ranges	$-13 \leqslant h \leqslant 13$ $-16 \leqslant k \leqslant 16$ $-17 \leqslant l \leqslant 17$
Reflections collected	62,289
Independent reflections	7026 [*R*(int) = 0.0236]
Completeness to 2*θ* = 27.00 (%)	99.3
Absorption coefficient (mm^{-1})	1.393
Refinement method	Full-matrix least-squares on F^2
Data/restraints/parameters	7026/0/449
Final *R* indices[a] [$I > 2\sigma(I)$][b]	$R_1 = 0.0362$, $wR_2 = 0.1033$
Goodness-of-fit on F^2[c]	0.995
R indices (all data)	$R_1 = 0.0406$, $wR_2 = 0.1096$
Largest difference in peak and hole (e Å^{-3})	0.597 and −0.633

[a] $R = \Sigma||F_o|-|F_c||/\sum|F_o|$.
[b] $wR = [(\sum[F_o^2 - F_c^2)^2]/\sum[w(F_o^2)^2]^{1/2}$.
[c] $S = \sum[w(F_o^2 - F_c^2)^2/(N_{obs} - N_{param})]^{1/2}$.

2.4. *X-ray structure determination*

The X-ray data for **1** were collected on a Bruker–Nonius X8 ApexII diffractometer equipped with a CCD area detector by using graphite-monochromated Mo Kα radiation ($\lambda = 0.71073$ Å) generated from a sealed tube source. Data were collected and reduced by SMART and SAINT software [34] in the Bruker package. The structure was solved by direct methods [35] and then developed by least-squares refinement on F^2 [36, 37]. The non-H atoms found in the electron density map were refined anisotropically. All hydrogens were placed in calculated positions with the "riding-model technique." Details concerning collection and analysis are reported in table 1.

2.5. *MLR analysis*

To explain the relationship between the maximum wavenumber of the complexes with the solvent parameters, SPSS/PC software package was used [38] and the best regression model was found by using the stepwise method. This method has a procedure in three

steps comprising identifying an initial model, adding and removing the parameters, and finally obtaining the best model which has higher R (multiple correlation coefficients) and F-values, lower standard error (SE), the least number of parameters and high ability for prediction [39]. The solvent parameters considered in this study for interpreting solute–solvent interactions are hydrogen bonding ability "α," electron pair donating ability "β," polarity/polarizability parameter "π^*" (measure of the ability of the solvent to stabilize a charge or a dipole by virtue of its dielectric effect), Gutmann's donor number "DN" (negative ΔH for a 1 : 1 adduct formation between $SbCl_5$ and solvent molecules in a dilute solution of 1,2-dichloroethane or dichloromethane), Mayer and Gutmann's acceptor number "AN" (derived from ^{31}P NMR of triethylphosphine oxide in different solvents) as well as Dimorth and Richardt's "$E_T(30)$" (molar electronic transition energy of dissolved negatively solvatochromic pyridinium N-phenolate betaine dye).

3. Results and discussion

Complex **1** was prepared by mixing *TAP*, *tmen*, $Cu(ClO_4)_2{\cdot}6H_2O$, and Na_2CO_3 with molar ratio of 1 : 2 : 2 : 1 in ethanol–water mixture as shown in equation (1). Complex **2** was synthesized with high yields by substitution of perchlorate with BPh_4^-.

$$\begin{aligned} &TAP + 2tmen + 2Cu(ClO_4)_2 \cdot H_2O + Na_2CO_3 \xrightarrow{H_2O/EtOH} [(tmen) \\ &\quad (CH_3CN)Cu(TAP)Cu(tmen)(ClO_4)]ClO_4 + CO_2 + 2NaClO_4 + 2H_2O \end{aligned} \quad (1)$$

Analytical data, molar conductivity values, IR spectra, and X-ray crystallography indicated formation of the desired mixed-chelate copper(II) complexes.

3.1. *X-ray structure*

A perspective view together with the atom labeling scheme for **1** is given in figure 1 and selected bond parameters are given in table 2. Each copper is surrounded by two nitrogen atoms of *tmen* and two oxygens of *TAP* chelates in the basal position and the fifth position

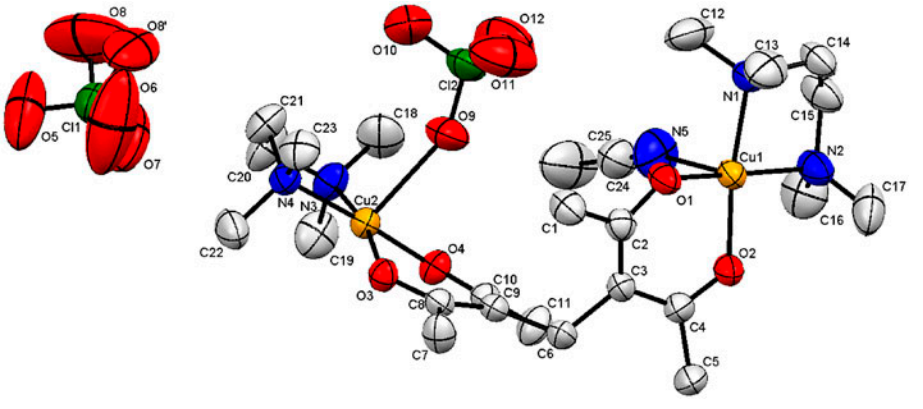

Figure 1. ORTEP view of **1**.

Table 2. Selected bond lengths (Å) and angles (°) for **1**.

Bond distances (Å)		Bond angles (°)	
N(1)–Cu(1)	2.046(2)	O(1)–Cu(1)–N(1)	89.79(9)
N(2)–Cu(1)	2.034(2)	O(1)–Cu(1)–N(2)	169.55(11)
O(1)–Cu(1)	1.8929(18)	N(1)–Cu(1)–N(2)	86.28(10)
O(2)–Cu(1)	1.9157(18)	N(1)–Cu(1)–O(2)	168.63(10)
N(3)–Cu(2)	2.053(2)	O(1)–Cu(1)–O(2)	89.82(8)
N(4)–Cu(2)	2.018(2)	O(2)–Cu(1)–N(2)	92.13(9)
O(3)–Cu(2)	1.9040(17)	N(1)–Cu(1)–N(5)	96.60(14)
O(4)–Cu(2)	1.8956(17)	O(1)–Cu(1)–N(5)	93.80(12)
C(2)–O(1)	1.275(3)	N(2)–Cu(1)–N(5)	96.27(12)
C(4)–O(2)	1.280(3)	O(3)–Cu(2)–N(3)	167.89(9)
C(2)–C(3)	1.403(3)	O(3)–Cu(2)–N(4)	91.98(8)
C(3)–C(4)	1.403(3)	N(3)–Cu(2)–N(4)	85.59(9)
C(8)–O(3)	1.288(3)	N(3)–Cu(2)–O(4)	91.16(9)
C(10)–O(4)	1.280(3)	O(3)–Cu(2)–O(4)	90.40(7)
C(8)–C(9)	1.400(3)	O(4)–Cu(2)–N(4)	174.93(8)
C(9)–C(10)	1.406(3)	O(3)–Cu(2)–O(9)	90.0(5)
N(5)–Cu(1)	2.334(3)	O(4)–Cu(2)–O(9)	90.4(6)
O(9)–Cu(2)	2.557(13)	N(3)–Cu(2)–O(9)	102.0(6)
		N(4)–Cu(2)–O(9)	94.0(6)
		C(3)-C(6)–C(9)	114.7(2)

is occupied by oxygen of perchlorate or nitrogen of acetonitrile. The dinuclear subunits are connected by bridging *TAP*. The structure contains a perchlorate counter ion that is free from coordination. The intradimeric Cu···Cu distance is 7.396(3) Å and interdimeric distance is 5.025 Å. According to Addison *et al.* [40], distortion of the square pyramidal geometry toward trigonal bipyramidal can be described by geometrical parameter $\tau = |\beta - \alpha|/60$ ($\tau = 0$ for ideal SP and 1 for ideal TBP), where β and α are the bond angles involving the *trans* donors in the basal plane. The τ value for coordination around Cu(1) and Cu(2) is 0.015 and 0.120, respectively, confirming square pyramidal geometry for both mononuclear subunits. The basal atoms are nearly coplanar; the deviations from the least-squares plane through CuN_2O_2 are N(1) 0.012, N(2) −0.012, O(1) 0.013, O(2) −0.012, Cu(1) 0.186 Å, and N(3) −0.066, N(4) 0.066, O(3) −0.068, O(4) 0.068, Cu(2) 0.138 Å, respectively. The Cu(1) and Cu(2) ions are displaced by 0.186(4) and 0.138(5) Å from the basal least square plane toward the apical atoms, respectively. The mean Cu–N(amine) distance of 2.03 Å and the bite angles N(1)–Cu–N(2) of 86.3(6)° and N(3)–Cu–N(4) of 85.5(6)° for the five-membered rings of *tmen* are close to the corresponding average values of reported copper(II) complexes with ethylenediamine [41, 42]. Both *TAE–Cu* rings have boat conformations. The angles between two six-membered rings of *TAP* are 56.81(5)° and twisted so that the dihedral angle C(2)–C(3)–C(6)–C(9) is 62.04°. The apical bond lengths Cu(1)–N(CH_3CN) of 2.334(3) Å and Cu(2)–O(ClO_4) of 2.557(13) Å are much longer than usual due to Jahn–Teller effect for d^9 electronic configuration. As a result, the apical groups are weakly coordinated to copper(II) and can be easily replaced by solvent molecules in solution leading to the observed solvatochromism.

3.2. *IR spectra*

The preparation of dinuclear mixed-chelate complexes also can be examined by infrared spectra analysis. Presence of characteristic bands of ligands and counter ions in the

Table 3. The molar conductivities (Λ_M) of **1** and **2** ($\Omega^{-1}\,cm^2\,M^{-1}$, at 25 °C) in some solvents.

Compound	DCM	MeOH	EtOH	ACN	ACO	DMF
1	47	195	88	285	216	145
2	51	203	–	266	195	140
1 : 2 electrolyte	–	160–220	79–90	220–300	160–200	130–170

complexes confirms the formation of the mixed-chelate complex. The C=O vibration of free TAP appears as a strong band at 1700 cm^{-1} but upon formation of the six-membered chelate rings this band moves to 1600 cm^{-1} in addition to changes in frequency of the C=O and C=C–C vibrations. The presence of ClO_4^- in **1** is shown by an intense and broad band at

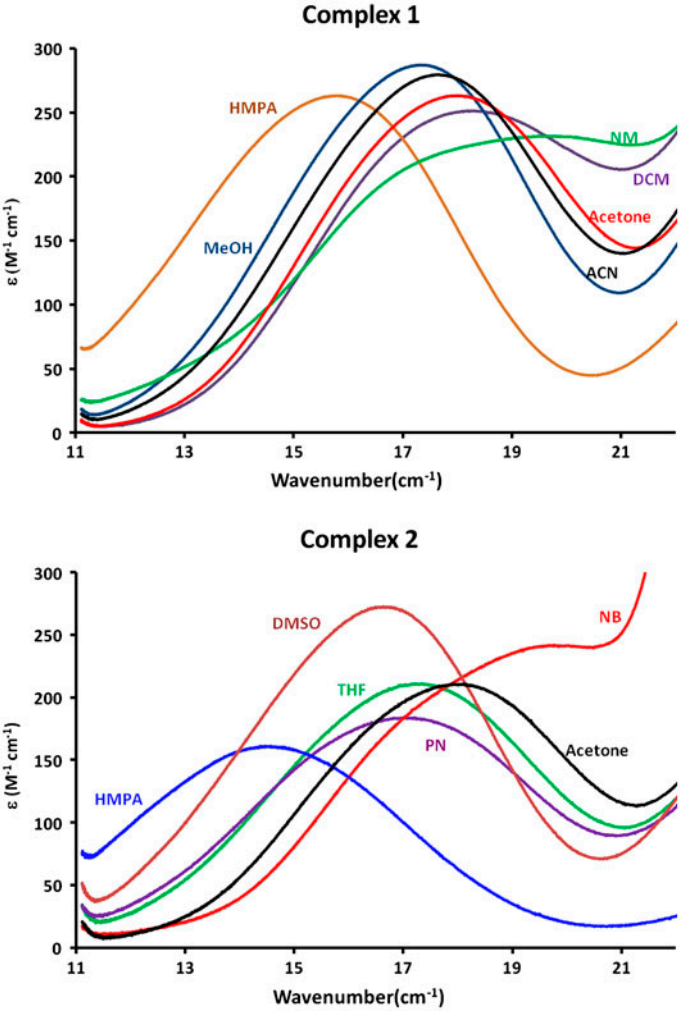

Figure 2. Absorption spectra of **1** and **2** in selected solvents.

1100 cm^{-1} and a sharp band with medium intensity at 610 cm^{-1} attributed to the anti-symmetric stretch and anti-symmetric bend, respectively. The existence of tetraphenylborate in **2** is revealed by intense absorptions at 720 and 750 cm^{-1} [43]. Spectra of **1** and **2** are shown in supplementary material. At lower frequency, the complexes exhibit bands at 503–512 and 480–490 cm^{-1} attributed to ν(Cu–O) and ν(Cu–N), respectively [44]. Due to the larger dipole moment change for Cu–O compared to Cu–N, ν(Cu–O) usually appears at higher frequency than ν(Cu–N) [45].

3.3. *Conductometric data*

The molar conductivity values of the complexes in some solvents have been studied, and the results with the standard values for 2 : 1 electrolytes in the respective solvents [46, 47] are in table 3. These results show that in solution the conductances of the complexes are in agreement with those expected for 1 : 2 electrolytes. Thus, counter ions are free from coordination even in dichloromethane with poor coordination ability.

3.4. *Solvatochromism*

The d–d absorption spectra of **1** and **2** in some solvents are presented in figure 2. Both complexes have good solubility in various organic solvents with different polarities. The

Table 4. The solvent parameter values and electronic absorption maxima of **1** and **2** in various solvents: ν_{max}/10^3 cm^{-1} (ε/M^{-1} cm^{-1}).

Solvent	DN	AN	$E_T(30)$	β	α	π^*	**1**	**2**
DCM	0.0	20.4	40.7	0.00	0.13	0.13	18.18 (251.56)	17.76 (–)
Nitromethane	2.7	20.5	46.3	0.06	0.22	0.85	16.96 (231.34)	17.79 (161.7)
Nitrobenzene	4.4	14.8	41.2	0.39	0.0	1.01	18.93 (259.58)	18.52 (–)
Benzonitryl	11.9	15.5	41.5	0.41	0.0	0.9	17.77 (254.28)	17.75 (206.75)
Acetonitrile	14.1	18.9	45.6	0.31	0.19	0.75	17.66 (279.38)	17.61 (196.35)
Propionitryl	16.1	16.0	43.6	0.39	0.0	0.71	17.42 (250.16)	17.07 (184.10)
Acetone	17.0	12.5	42.2	0.48	0.08	0.71	17.99 (263.54)	17.92 (211.25)
MeOH	19.0	41.3	55.4	0.62	0.9	0.6	17.32 (287.58)	17.05 (219.95)
THF	20.0	8.0	37.4	0.55	0.0	0.58	–[a]	17.21 (211.45)
EtOH	20.0	37.1	51.9	0.77	0.86	0.75	17.16 (286.56)	–[a]
DMF	26.6	16.0	43.2	0.69	0.0	0.88	16.86 (258.32)	16.85 (220.35)
DMSO	29.8	19.3	45.1	0.76	0.0	1.0	16.62 (157.96)	16.63 (272.95)
Py	33.1	14.2	40.5	0.64	0.0	0.87	15.51 (167.35)	15.43 (150.3)
HMPA	38.8	10.6	40.9	1.05	0.0	0.87	15.87 (263.40)	14.58 (161.45)
$\Delta\nu_{max}$ (cm^{-1})							3750 cm^{-1}	3770 cm^{-1}

[a]The compound is almost insoluble.

Table 5. The equations from the linear correlation of ν_{max} with DN of the solvents[a].

Complex number	Equation[b]	F	SE	R
1	$\nu_{max} = -0.089\ (\pm0.012)DN_{solv} + 19.051\ (\pm0.245)$	59.2	0.471	0.918
2	$\nu_{max} = -0.091\ (\pm0.013)DN_{solv} + 18.808\ (\pm0.292)$	47.7	0.479	0.909

[a]Based on 13 data points (solvents) indicated in table 4.
[b]Data in parentheses are standard error (SE).

observed frequencies of the d–d absorptions (ν_{max}) of each complex along with the molar absorptivity and their respective solvent parameter values from literature [27, 48] are illustrated in table 4. This band arises from transition to the $d_{x^2-y^2}$ orbital of the copper(II). The energy change in absorption spectra of **1** and **2** (table 4) is as large as 3700–3750 cm^{-1} over the solvents studied. The two complexes show solvatochromic behavior with the counter ion playing a weak role in the position of ν_{max} of the complexes.

The SMLR method was carried out to determine the main solvent parameters that influence the d–d absorption (ν_{max}) of the complexes; the solvatochromic equation (2) was used. In this equation, *a–f* are the solvent-independent coefficients, characteristic of the process, and indicative of its sensitivity on the accompanying solvent properties.

$$\nu_{max} = \nu^{\circ}_{max} + a\mathrm{DN} + b\alpha + c\beta + d\pi^{*} + e\mathrm{AN} + fE_T(30) \quad (2)$$

Due to the correlation results of the absorption frequencies with the solvent parameters, table 5, the DN parameter has a dominant contribution to the shift of ν_{max} of the

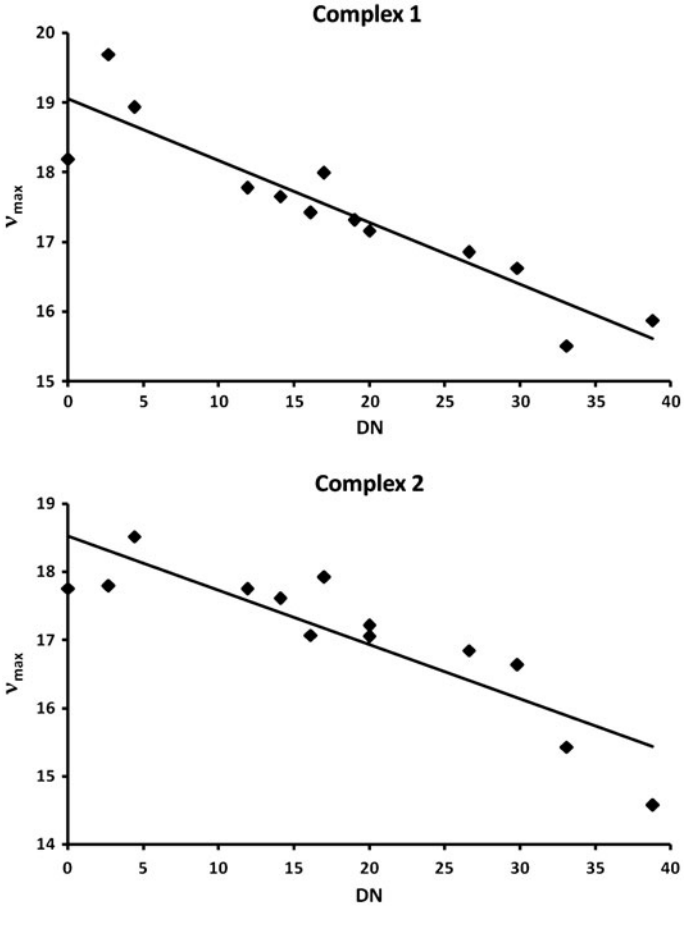

Figure 3. Dependence of the ν_{max} of the complexes on the solvent DN.

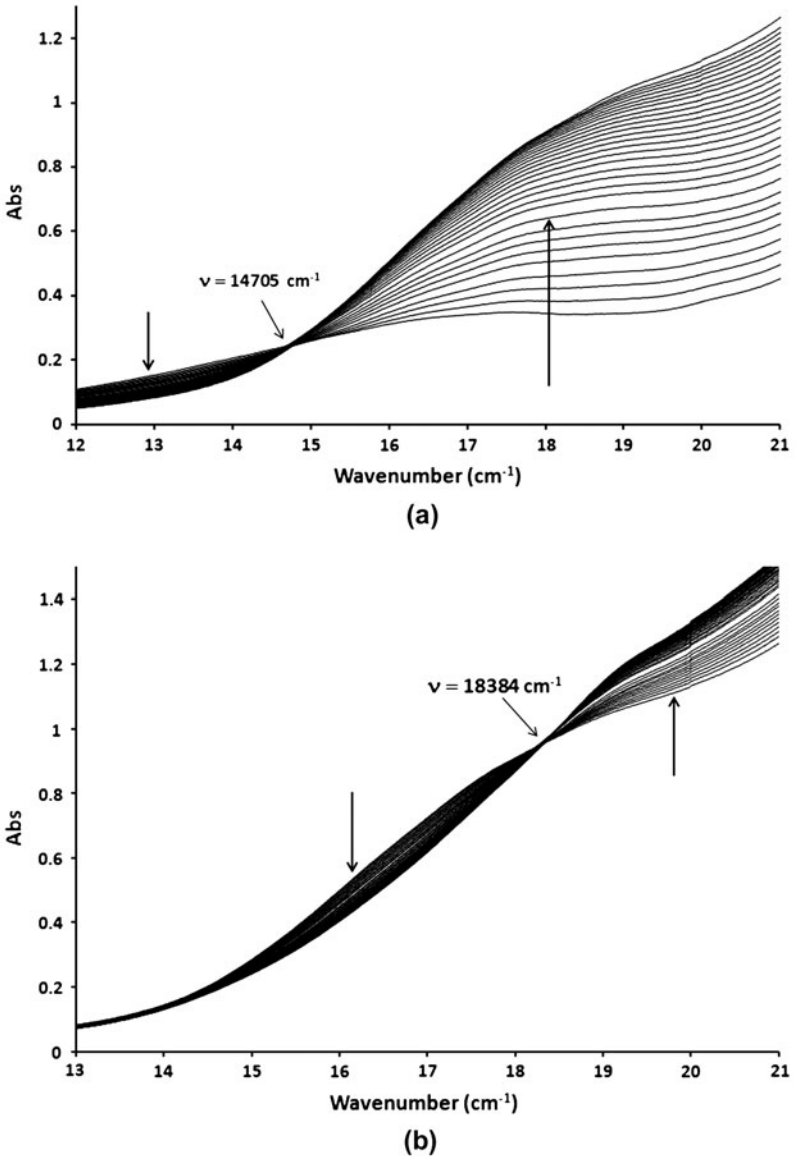

Figure 4. Spectral changes of **1** (4.0×10^{-3} M dm^{-3}) in pyridine at 25 °C during (a) the first 160 min and (b) the next 160 min.

complexes. The contribution of the other solvent parameters was negligible and rejected based on statistical criteria explained in the experimental section. This exploration is further corroborated by the linearity of ν_{max} (cm^{-1}) values of the complexes in different solvent versus the DN of the solvents (figure 3).

In pyridine for both complexes, the original green color of the solution turns dark brown over 320 min at room temperature. To investigate, this color change visible spectra of the

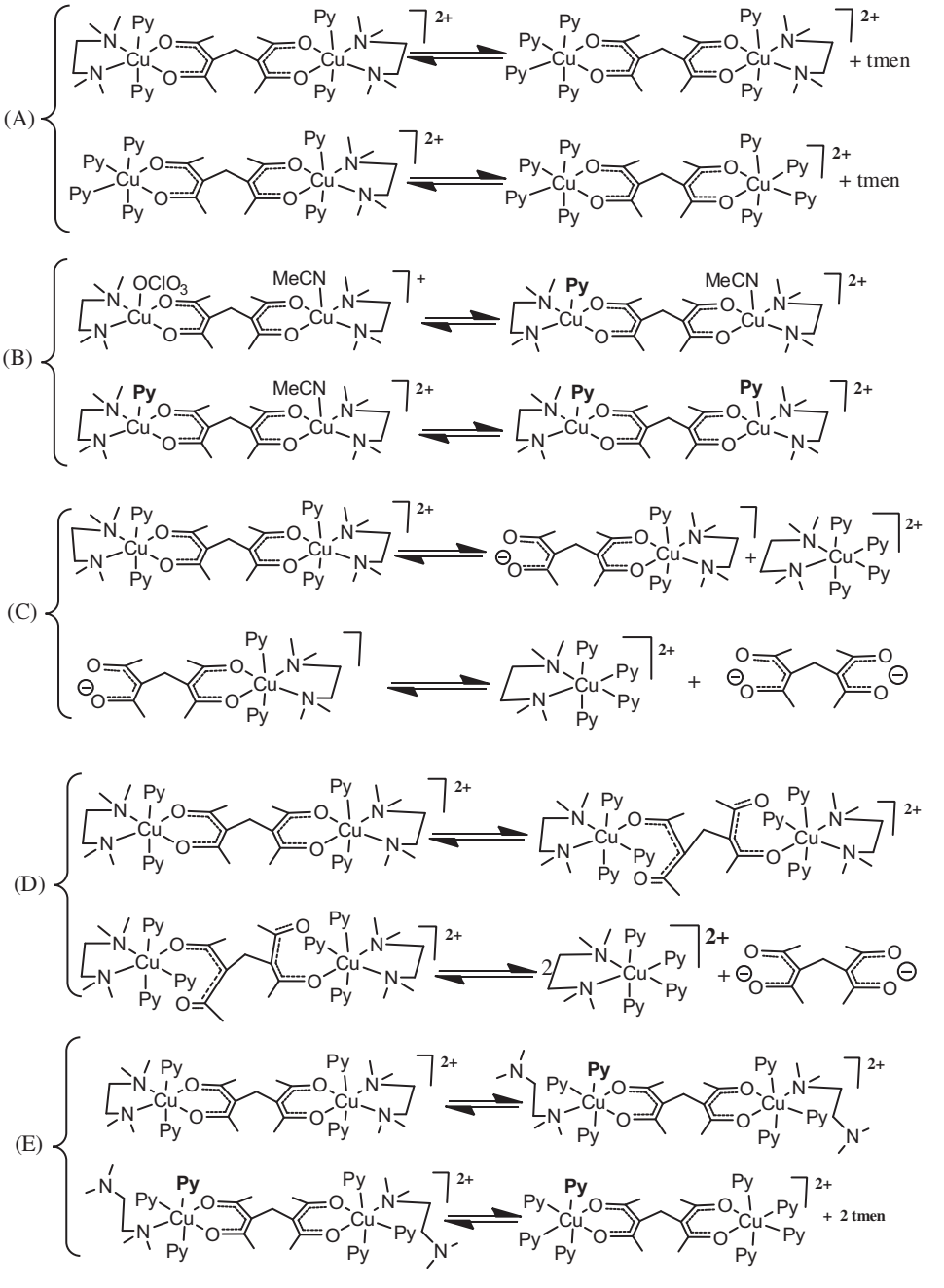

Scheme 2. The possible mechanisms for observed spectral changes.

complex were studied over time. These results are shown in figure 4. There are two isosbestic points at 14,705 and 18,384 cm^{-1} which became visible in different time scales. The former appeared during the time interval of 0–160 min while the latter emerged during

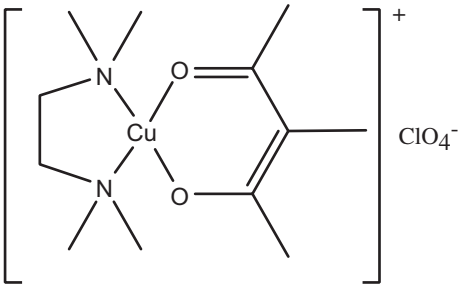

Scheme 3. The mononuclear mixed-chelate complex.

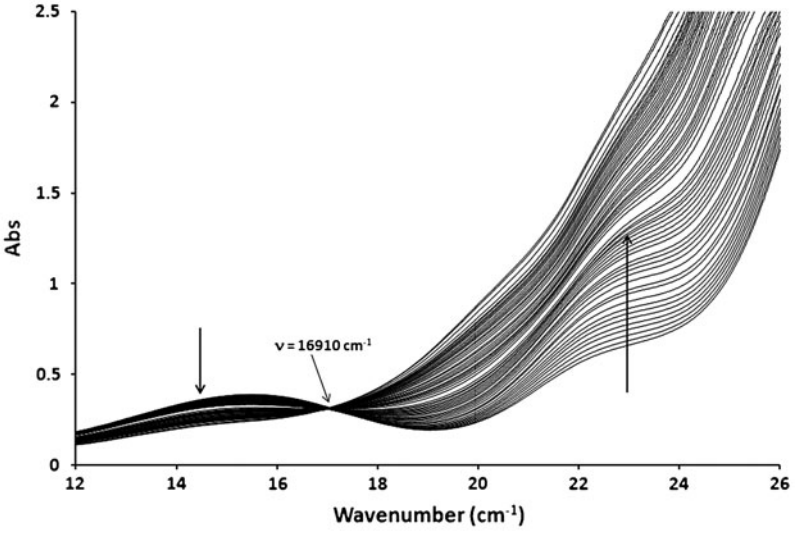

Figure 5. Spectral changes of **3** (5.0×10^{-3} M dm^{-3}) in pyridine at 25 °C 7 h after preparation.

160–320 min (figure 4) and no change in the spectra happened afterward. During the appearance of the first isosbestic point at 14,705 cm^{-1}, the absorption at 15,625 cm^{-1} remains intact along with appearance of new peaks between 20,000 and 16,666 cm^{-1} that obscure the weaker absorption at 15,625 cm^{-1}. Unfortunately, these absorptions can hardly be resolved. It seems that during this time interval, the electronic environment of the copper centers in the complexes is changed and two unsymmetrical copper(II) centers are generated. Interestingly, after 160 min, the first isosbestic point vanished and the second isosbestic point emerged and the electronic transitions around 18,200 and 15,400 cm^{-1} disappeared with the transition at 19,200 cm^{-1} becoming visible. Each of these isosbestic points is from equilibria between two species in solution. There are several possibilities for this phenomenon that are presented in scheme 2.

The former isosbestic point is assigned to dissociation of one *tmen* chelate of the solvated complex that was substituted by pyridine, and the latter isosbestic point is referred to the dissociation of the next *tmen* chelate which was replaced with pyridine, as shown in equilibria A presented in scheme 2. The solvation equilibria of type (B) that are associated to

substitution of weakly coordinated acetonitrile and perchlorate by solvent molecules (scheme 2) were excluded because of the lack of change in the conductivity of the solution over time. Additionally, even in weak donor solvents such as dichloromethane, nitromethane, and nitrobenzene, solvation occurs rapidly in freshly prepared solution (see figure 3). Other possible mechanisms could be the presence of equilibria type (C) or (D). These routes were eliminated since the conductivity of the solution remained constant over time. To confirm the proposed mechanism (A), an excess of *tmen* (*ca.* equimolar with pyridine) was added to the freshly prepared solution to drive the equilibria to the left. The reaction was apparently suppressed and no color change or isosbestic point was observed after several days. To rule out equilibria type (E), the mononuclear copper complex **3** was studied (scheme 3). The results are illustrated in figure 5. As expected, only an isosbestic point was observed at 16,910 cm^{-1} and the conductivity of the mononuclear complex was unchanged after several days. If the equilibria type (E) exists in mononuclear complex, two isosbestic points rather than one would be expected. Removal of each *tmen* can proceed in two successive steps but bond rupture of one end of a chelate is much faster than the second bond breakage and removal of a chelate from coordination sphere due to high kinetic stability of the chelate [49]. Heating of the solution accelerates the time to a few minutes.

4. Conclusion

Two new dinuclear mixed-chelate copper(II) complexes with solvatochromic properties was prepared. Their solvatochromism were tested with different solvent parameter models using the SMLR computational method. The statistical evaluation of the data (*R*, SE., and *F*-test) indicated that DN of the solvent plays the most important role in solvatochromic behavior of the complexes. The d–d band of the compounds exhibited a red shift with increase in DN of solvent. The dinuclear mixed–chelate complexes showed more solvatochromism than mononuclear counterparts with higher molar absorptivity. The $\Delta\nu_{max}$ for complexes is as large as 3750 cm^{-1}; $\Delta\nu_{max} = (\nu_{max})DCM - (\nu_{max})HMPA$. The X-ray analysis of **1** indicated square pyramidal copper centers with CuN_2O_2 in the basal plane and apical positions occupied by perchlorate in one site and acetonitrile at the other. In solvation, the geometries of the complexes change from square pyramidal to octahedral. In pyridine, the original green color of the solution turns dark brown over time due to elimination of diamine and substitution with pyridine in two consecutive steps.

Supplementary data

CCDC 917648 contains the supplementary crystallographic data for this paper. These data can be obtained free of charge via http://www.ccdc.cam.ac.uk/conts/retrieving.html or from the Cambridge Crystallographic Data Centre, 12 Union Road, Cambridge CB2 1EZ, UK; Fax: (+44) 1223 336033; or E-mail: deposit@ccdc.cam.ac.uk.

Acknowledgment

We are grateful for the financial support of the University of Mazandaran of the Islamic Republic of Iran.

References

[1] P.A. Vigato, V. Peruzzo, S. Tamburini. *Coord. Chem. Rev.*, **253**, 1099 (2009).
[2] N. Shintani, J. Kutaki, K. Sone, Y. Fukuda. *Bull. Chem. Soc. Jpn.*, **66**, 784 (1993).
[3] K. Miyamoto, M. Sakamoto, C. Tanaka, E. Horn, Y. Fukuda. *Bull. Chem. Soc. Jpn.*, **78**, 1061 (2005).
[4] L. Rigamonti, F. Demartin, A. Forni, S. Righetto, A. Pasini. *Inorg. Chem.*, **45**, 10976 (2006).
[5] W. Linert, Y. Fukuda, A. Camard. *Coord. Chem. Rev.*, **218**, 113 (2001).
[6] Y. Fukuda, K. Sone. *Bull. Chem. Soc. Jpn.*, **45**, 465 (1972).
[7] Y. Fukuda, A. Shimura, M. Mukaida, E. Fujita, K. Sone. *J. Inorg. Nucl. Chem.*, **36**, 1265 (1974).
[8] Y. Fukuda, Y. Miura, K. Sone. *Bull. Chem. Soc. Jpn.*, **50**, 154 (1977).
[9] Y. Fukuda, N. Sato, N. Hoshino, K. Sone. *Bull. Chem. Soc. Jpn.*, **54**, 428 (1981).
[10] R.W. Soukup, R. Schmid. *J. Chem. Educ.*, **62**, 459 (1985).
[11] Y. Fukuda, Y. Miura, K. Sone. *Bull. Chem. Soc. Jpn.*, **50**, 142 (1977).
[12] Y. Fukuda, H. Okamura, K. Sone. *Bull. Chem. Soc. Jpn.*, **50**, 313 (1977).
[13] Y. Fukuda, K. Sone. *Bull. Chem. Soc. Jpn.*, **58**, 3518 (1985).
[14] Y. Fukuda, M. Cho, K. Sone. *Bull. Chem. Soc. Jpn.*, **62**, 51 (1989).
[15] H. Golchoubian, E. Rezaee, G. Bruno, H.A. Rudbari. *Inorg. Chim. Acta*, **366**, 290 (2011).
[16] H. Golchoubian, E. Rezaee. *J. Mol. Struct.*, **927**, 91 (2009).
[17] H. Golchoubian, G. Moayyedi, H. Fazilati. *Spectrochim. Acta, Part A*, **85**, 25 (2012).
[18] H. Golchoubian, G. Moayyedi, G. Bruno, H.A. Rudbari. *Polyhedron*, **30**, 1027 (2011).
[19] H. Golchoubian, E. Rezaee. *J. Mol. Struct.*, **929**, 154 (2009).
[20] H. Golchoubian, E. Rezaee, G. Bruno, H.A. Rudbari. *Inorg. Chim. Acta*, **394**, 1 (2013).
[21] K. Sone, Y. Fukuda. *Rev. Inorg. Chem.*, **11**, 123 (1990).
[22] K. Sone, Y. Fukuda. *Inorganic Thermochromism*. In *Inorganic Chemistry Concepts*, Vol. 10, Springer, Berlin (1987).
[23] Y. Fukuda, K. Sone. *J. Inorg. Nucl. Chem.*, **34**, 2315 (1972).
[24] R. Yamamoto, T. Maruyama. *Jpn. Kokai Tokyo Koho, JP*, 06073169 (1994).
[25] O. Sato, S. Hayami, Y. Einaga, Z-Z Gu. *Bull. Chem. Soc. Jpn.*, **76**, 443 (2003).
[26] K.S. Schanze, R.H. Schmehl. *J. Chem. Educ.*, **74**, 633 (1997).
[27] V. Gutmann. *Coordination Chemistry in Non-aqueous Solutions*, Springer, Vienna (1968).
[28] V. Gutmann. *The Donor–Acceptor Approach to Molecular Interactions*, Plenum Press, New York (1978).
[29] W. Linert, V. Gutmann. *Coord. Chem. Rev.*, **117**, 159 (1992).
[30] W. Mizerski, M.K. Kalinowski. *Monatsh. Chem.*, **123**, 675 (1992).
[31] Y. Marcus. *Chem. Soc. Rev.*, **22**, 409 (1993).
[32] S. Burton, F.R. Fronczek, A.W. Maverick. *Acta Cryst.*, **E63**, O3108 (2007).
[33] H. Asadi, H. Golchoubian, R. Welter. *J. Mol. Struct.*, **779**, 30 (2005).
[34] Bruker AXS Inc. *SMART (Version 5.060) and SAINT (Version 6.02)*, Madison, Wisconsin, USA (2007).
[35] M.C. Burla, R. Caliandro, M. Camalli, B. Carrozzini, G.L. Cascarano, L. De Caro, C. Giacovazzo, G. Polidori, R. Spagna. *J. Appl. Cryst.*, **38**, 381 (2005).
[36] G.M. Sheldrick. *SHELXL97, Program for Crystal Structure Refinement*, University of Göttingen, Germany (2008).
[37] *SHELXT LN. Version 5.10*, Bruker Analytical X-ray Inc., Madison, Wiskonsin, USA (2008).
[38] SPSS/PS. *Statistical package for IBMPC, Quiad software version 13*, Ontario (1998).
[39] S. Riahi, M.F. Mousavi, M. Shamsipur. *Talanta*, **69**, 736 (2006).
[40] A.W. Addison, T.N. Rao. *J. Chem. Soc., Dalton Trans*., 1349 (1984).
[41] H. Golchoubian. *Anal. Sci.*, **24**, x169 (2008).
[42] H. Golchoubian. *Anal. Sci.*, **24**, x195 (2008).
[43] N. Sekine, T. Shiga, M. Ohba, H. Okawa. *Bull. Chem. Soc. Jpn.*, **79**, 881 (2006).
[44] N. Raman, S. Esthar, C. Thangaraja. *J. Chem. Sci.*, **116**, 209 (2004).
[45] N. Chkaku, K. Nakamoto. *Inorg. Chem.*, **10**, 798 (1971).
[46] W.J. Geary. *Coord. Chem. Rev.*, **7**, 81 (1971).
[47] M. Yonemura, K. Arimura, K. Inoue, M. Ohaba, H. Okawa. *Inorg. Chem.*, **41**, 582 (2002).
[48] V. Gutmann. *Coord. Chem. Rev.*, **18**, 225 (1976).
[49] R.G. Wilkins. *Kinetics and Mechanism of Reaction of Transition Metal Complexes*, 2nd Edn, p. 219, Wiley-VCH, Weinheim (2002).